ACS APPLIED MATERIALS & INTERFACES

Research Article

www.acsami.org

Ionic-Liquid-Based Proton Conducting Membranes for Anhydrous H_2/Cl_2 Fuel-Cell Applications

Sa Liu,[†,‡] Li Zhou,*[,†] Pengjie Wang,[†,‡] Fangfang Zhang,[†,‡] Shuchun Yu,[†,‡] Zhigang Shao,*[,†] and Baolian Yi[†]

[†]Fuel Cell System and Engineering Laboratory, Dalian Institute of Chemical Physics, Chinese Academy of Sciences, 457 Zhongshan Road, Dalian 116023, China

[‡]University of Chinese Academy of Sciences, Beijing 100039, China

Supporting Information

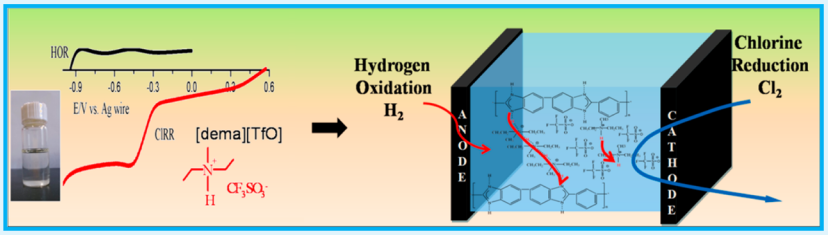

ABSTRACT: An ionic-liquid-doped poly(benzimidazole) (PBI) proton-conducting membrane for an anhydrous H_2/Cl_2 fuel cell has been proposed. Compared with other ionic liquids, such as imidazole-type ionic liquids, diethylmethylammonium trifluoromethanesulfonate ([dema][TfO]) showed better electrode reaction kinetics (H_2 oxidation and Cl_2 reduction reaction at platinum) and was more suitable for a H_2/Cl_2 fuel cell. PBI polymer and [dema][TfO] were compatible with each other, and the hybrid membranes exhibited high stability and good ionic conductivity, reaching 20.73 mS cm^{-1} at 160 °C. We also analyzed the proton-transfer mechanism in this ionic-liquid-based membrane and considered that both proton-hopping and diffusion mechanisms existed. In addition, this composite electrolyte worked well in a H_2/Cl_2 fuel cell under non-water conditions. This work would give a good path to study the novel membranes for anhydrous H_2/Cl_2 fuel-cell application.

KEYWORDS: *ionic liquid, poly(benzimidazole), polymer composite membrane, nonhumidified fuel cell*

INTRODUCTION

A fuel cell is an excellent alterative to an internal combustion engine, particularly because of its ecofriendly nature and high-energy utilization efficiency.[1] Although comparatively less popular than the H_2/O_2 polymer electrolyte membrane fuel cell (PEMFC), the H_2/Cl_2 fuel cell was reported as an alternative in the early 1920s in the chlorine−alkaline industry, space applications, and regenerative systems for energy storage.[2,3] In marked contrast to the H_2/O_2 fuel cells, in which sluggish oxygen reduction kinetics leads to substantial activation overpotential, H_2/Cl_2 fuel cells are able to operate with little activation loss associated with the chlorine electrode because of relatively facile chlorine redox kinetics.[4,5] In the H_2/Cl_2 fuel cells, owing to the high hydrophilicity of the product hydrogen chloride, most of the water will be removed from the cell, and this causes an increase in the membrane resistance and a decrease in the cell performance.[6] In general, the resource is keeping chlorine gas dissolved in hydrochloric acid[7−10] or applying a composite aqueous acid/Nafion electrolyte.[6,11,12] However, hydrochloric acid dramatically results in the corrosion of materials, and the cell performance is restricted by mass-transport limitation due to the limited solubility of chlorine in the acid. Hence, the best strategy should be to minimize the existence of liquid water. A phosphoric-acid-doped poly(benzimidazole) (PA/PBI) composite membrane was excellently suitable for high-temperature H_2/O_2 fuel cells under anhydrous conditions.[13,14] However, Thomassen et al. found that phosphoric acid was polymerized to pyrophosphoric acid or higher oligomers in the H_2/Cl_2 fuel cell,[6] drastically decreasing the membrane conductivity because hydrogen chloride forced water to be removed from the PBI/H_3PO_4 membrane during fuel-cell operation.

Ionic liquids (ILs) have received much attention because of their low vapor pressure, wide electrochemical windows, high chemical and thermal stability, and good ion conductivity.[15−17] Therefore, IL-based solid electrolytes were widely studied for high-temperature anhydrous fuel cells.[18−26]

Considering the above unique properties of ILs and the special operation conditions of the H_2/Cl_2 fuel cell, recently we first proposed a totally new design for the H_2/Cl_2 fuel-cell application,[27] employing a superabsorbent material absorbing IL to form a proton-conducting membrane. This electrolyte membrane worked well in the H_2/Cl_2 fuel cell under non-water conditions. However, IL was only physically absorbed in the

Received: October 22, 2013
Accepted: February 3, 2014
Published: February 3, 2014

membrane matrix. To further improve the stability of the composite membrane, solving the problem of IL leaching is a major consideration.

In this work, we prepared the PBI/diethylmethylammonium trifluoromethanesulfonate ([dema][TfO]) composite membranes with high retention of the IL and studied the characterization of the membrane and IL for the H_2/Cl_2 fuel cells under nonhumidified conditions.

EXPERIMENTAL SECTION

Materials. Poly(phosphoric acid) (PPA; 80% P_2O_5), P_2O_5 (98%), and triphenyl phosphate (TPP; 98%) were chemically pure commercial products. 3,3′-Diaminobenzidine (DABD; 99%, Aldrich) and isophthalic acid (IPA; 98%, Aldrich) were dried at 120 °C before the reaction. ILs were all obtained from Lanzhou Institute of Chemical Physics, CAS. *N*,*N*-Dimethylformamide (DMF; >99%) was supplied by Tianjing Fuyu Chemical Ltd., China.

Fabrication of PBI/IL Composite Membranes. PBI was synthesized as reported in refs 28 and 29 according to Scheme 1a.

Scheme 1. (a) PBI Synthesis Route and (b) Chemical Structure of [dema][TfO]

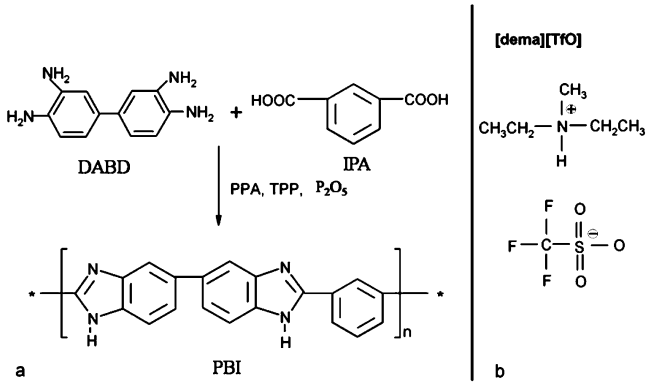

The membrane was prepared by the solution-casting method as follows: the homogeneous solution including IL, PBI resin, and DMF was cast on a glass matrix and dried at 80 °C for 24 h. The membranes were named PBI/[dema][TfO]*x*, where *x* was the IL content (wt %) in the composite membrane.

Electrochemical Characterization. The behavior of H_2 oxidation reaction (HOR) and Cl_2 reduction reaction (ClRR) in an IL was studied by a cyclic voltammetry (CV) method[20] at 120 °C under a N_2, H_2, or Cl_2 gas atmosphere. Platinum wire, silver wire, and platinum sheet were used as the working, reference, and counter electrodes, respectively. The CV curves were recorded at a rate of 20 mV s^{-1} using an CHI600C electrochemical workstation.

The effect of IL on the activity area of the Pt/C catalyst was evaluated as our early report (details are given in the Supporting Information, SI).[27]

Characterization. Fourier transform infrared (FTIR) was conducted using a spectrometer (Avatar 370 ESP).

The ionic conductivity of the IL was tested by a conductivity meter (DSA-11, Shanghai LEI-CI Co. Ltd., China) at different temperatures. To minimize experimental error, the measurement system was thermally stable at each temperature for 3 h before the measurements.

The conductivities of the hybrid membranes were measured by the alternating-current impedance method as in our previous work.[9]

Differential scanning calorimetry (DSC) was carried out on a Seiko Instrument DSC 811 under a N_2 gas atmosphere. The sample was heated to 150 °C, then cooled to −60 °C, and heated again to 150 °C at rate of 10 °C min^{-1}.

The thermal stability was measured by thermogravimetric analysis (TGA; STA449F3, Netzsch, Germany) at rate of 10 °C min^{-1} under an air atmosphere.

Membrane Electrode Assembly (MEA) Fabrication. The ionomer−PBI gas diffusion electrode (GDE) was used in this study, which was prepared as reported previously[29] (details in the SI). A membrane was sandwiched between two GDEs to form MEA with an active area of 5 cm^2.

Single-Cell Tests. Dry H_2 and Cl_2 gases were supplied to the fuel cell at ambient pressure. The fuel-cell polarization curve was determined by using an electronic load PLZ-50F (Kikusui, Japan), and the current density response to various cell voltage levels was monitored until steady-state conditions. The hydrogen-permeation current density at 120 °C was measured by applying a positive voltage (0.25 V vs NHE) at the cathode (while flushing it with nitrogen), oxidizing the hydrogen that permeated from the anode to the cathode.

RESULTS AND DISCUSSION

As candidates for the fuel-cell electrolytes, many kinds of ILs were considered,[18,20,30−32] such as pyridine-, imidazole-, and amine-based ILs. The imidazole-based ILs were most intensively investigated.[22,33−37] However, most of them have not provided fuel-cell performance, and a few of the papers gave the highest cell current density of less than 10 mA cm^{-2} and low open-circuit voltage.[35] To better understand the ILs as H_2/Cl_2 fuel-cell electrolytes, we focused on the HOR and ClRR at platinum in the ILs. Typical results were shown in Figure 1 (more results in Figures S1−S4 in the SI). When hydrogen was into the IL [dema][TfO], a HOR current sharp appeared at

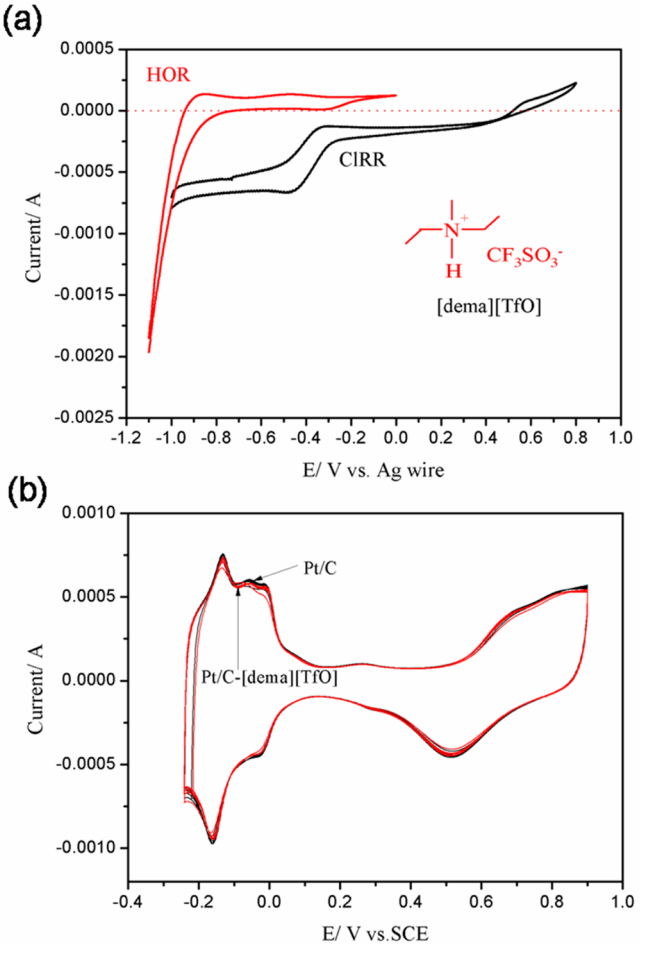

Figure 1. (a) CV curves for HOR and ClRR in [dema][TfO] at 120 °C under nonhumidification conditions. (b) CV curves of a blank Pt/C electrode and a Pt/C electrode dyed with [dema][TfO].

dx.doi.org/10.1021/am404645c | ACS Appl. Mater. Interfaces 2014, 6, 3195−3200

about −0.940 V (Figure 1a; this value was shifted to more negative than that reported by Walsh et al.,[38] possibly because of the different test system), clearly demonstrating that it supported activity H_2 oxidation in [dema][TfO], as reported by Watanabe et al.[20] While a striking difference was seen for other ILs, there was more overpotential (Figure S1a−S4a in the SI). When chlorine gas was bubbled into [dema][TfO], it could obviously see a ClRR current at about 0.574 V. It should be noted that the Cl_2 reduction rate in [dema][TfO] was generally greater than that in other ILs, which can be seen from the higher onset potential and slope of the polarization curve (Figures S1−S4 in the SI). These illuminated that [dema]-[TfO] gave the best results for the facile H_2 oxidation and Cl_2 reduction. As shown in the effect of ILs on the activity of platinum (Figures 1b and S1b−S4b in the SI), the less effect of [dema][TfO] on the platinum activity area,[27] compared with other ILs, appeared to be responsible for the better electrode performance.

In the experiment, we evaluated many polymers, such as Nafion, poly(vinylidene fluoride) and sulfonated poly(ether ether ketone), and found that PBI polymer showed the best compatibility with [dema][TfO]. Transparent, yellowish, free-standing, and flexible composite membranes (Figure 2) were obtained.

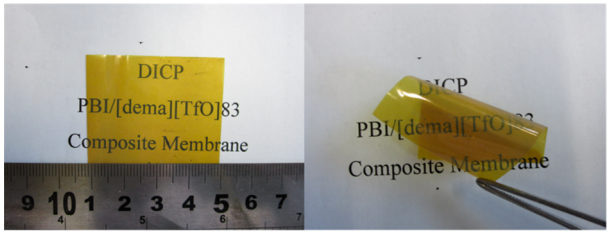

Figure 2. Photograph of the PBI/[dema][TfO]83 composite membrane.

The FTIR spectra are revealed in Figure 3. The PBI film exhibited characteristic absorption bands at 1668 and 3014−3370 cm^{-1} due to the group of C═N and N−H stretching vibrations, respectively. In addition, the absorption band at 1453 cm^{-1} was assigned to the stretching modes of the imidazole ring (C−C). Similar to the PBI membrane, the PBI/[dema][TfO] composite membrane also exhibited a peak at 3014−3370 cm^{-1} and the intensity of the peak did not change, illuminating no bonding between $[TfO]^-$ of [dema][TfO] and the N−H group of the PBI matrix.[39] However, with an increased amount of [dema][TfO], the intensity of the stretching vibrations of C═N at 1668 cm^{-1} and the imidazole ring at 1453 cm^{-1} decreased, indicating that there may be a strong interaction between C═N of PBI and H−N from the ammonium cations of [dema][TfO] and imide groups at the imidazole may be protonated by the IL. This interaction mode was different from that reported by Scott et al.[39] and Wang and Hsu.[40] The spectrum of [dema][TfO] showed various characteristic peaks associated with the IL structure. The peak at around 1033 cm^{-1} most likely resulted from the symmetric stretching vibration of the O═S═O group. The slight peak at 2515 cm^{-1} might be from the N^+−H bond stretching vibration. Two peaks at 2815 and 3071 cm^{-1} were C−H of the alkyl group stretching vibration. These characteristic peaks of [dema][TfO] also showed in the PBI/[dema][TfO] composite membranes.

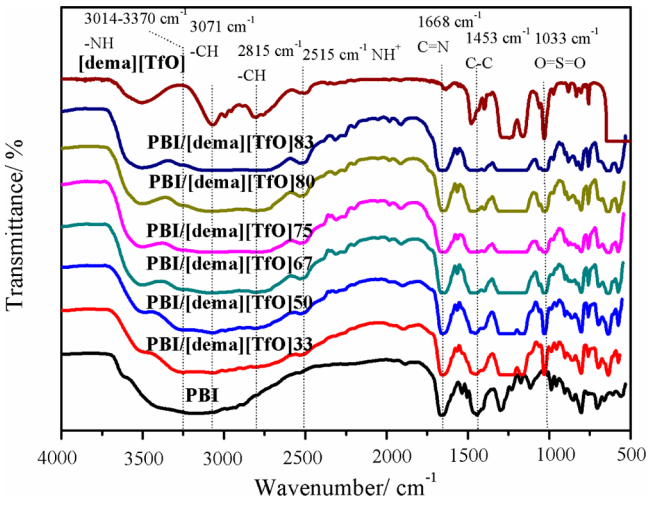

Figure 3. FTIR spectra of membranes and [dema][TfO].

The thermal stability was investigated by TGA, as shown in Figure 4. The 5% and 10% weight losses of the PBI membrane occurred at temperatures of about 125.67 and 230.40 °C, respectively. The decomposition temperature of PBI was lower than that reported in the literature,[29] which may be due to the little solvent residues during the synthesis of PBI and the bound water in the membrane. However, the composite membranes showed higher degradation temperature with the addition of [dema][TfO], which were all over 200 °C. This was because of the high thermal stability of [dema][TfO]. All of the composite membranes exhibited greater thermal stability than that of the PBI/H_3PO_4 system; the latter was decomposed to $H_4P_2O_7$ at 160 °C.[41] The above results illuminated that the prepared membrane had enough thermal stability to be used at high temperature (100−200 °C).

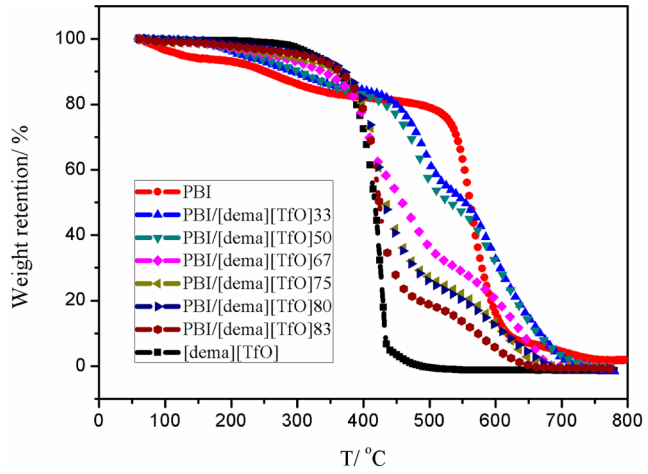

Figure 4. TGA curves of composite membranes and [dema][TfO].

As shown in the DSC thermograms (Figure 5), the endothermic peak representing free [dema][TfO] melting[26] was not found in the membranes including 33 wt %, 50 wt %, and 67 wt % [dema][TfO]. This indicated that the IL and PBI polymer matrix fully interacted with each other (as described in the FITR). However, the peak began to appear when the IL content further increased, which demonstrated that a little free

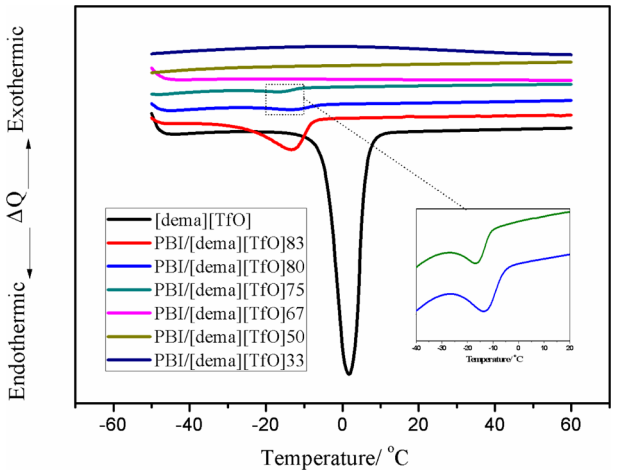

Figure 5. DSC thermograms for the IL and membranes.

IL remained inside the structure of the PBI film at the higher [dema][TfO] content.

The ionic conductivity (σ) of composite membranes and pure [dema][TfO] under anhydrous conditions is shown in Figure 6a. It can be seen that [dema][TfO] had high conductivity, which reached up to 70.50 mS cm^{-1} at 160 °C and still remained at 10.15 mS cm^{-1} at 30 °C. The PBI/[dema][TfO]33 and PBI/[dema][TfO]50 membranes exhibited low conductivity (<10^{-4} S cm^{-1} even at 160 °C; the date of the PBI/[dema][TfO]33 membrane was lower and is not shown), while the membranes exhibited reasonably high conductivity (>10^{-3} S cm^{-1} at 40 °C) when the [dema][TfO] content was further increased. Very high conductivity at a high content of the IL may be explained by enhanced free ionic mobility in the membrane matrix[42] and forming well-developed ionic channels. PBI/[dema][TfO] composite membranes prepared in this study showed conductivity comparative to that of reported membranes (Table S1 in the SI), suggesting that the composite membranes could be promising candidates for high-temperature application under anhydrous conditions such as PEMFC.

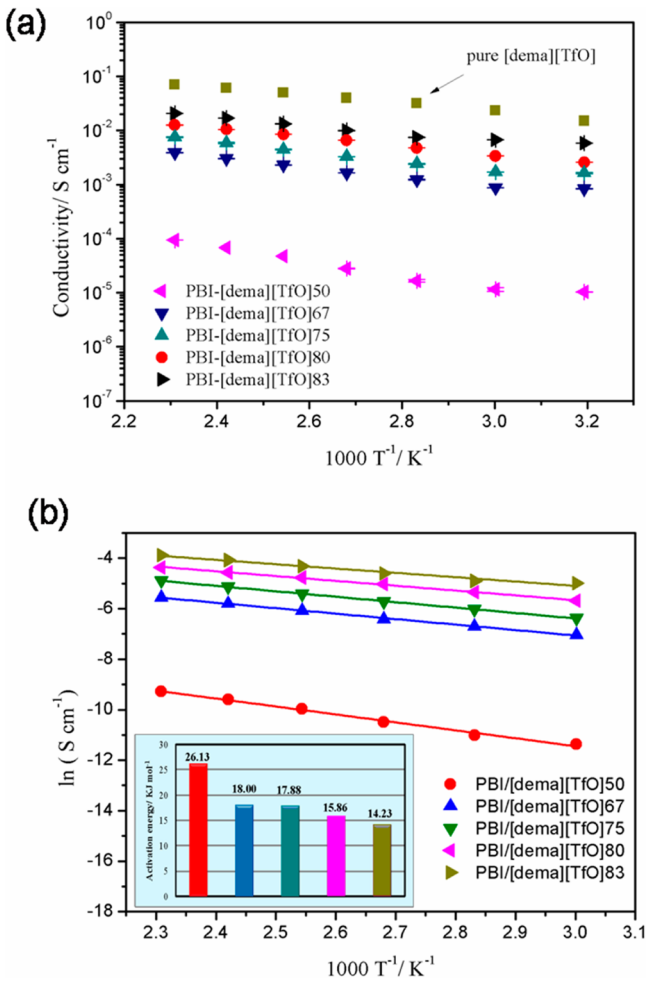

Figure 6. (a) Variation of the conductivity of the IL and membranes at different temperatures. (b) Curve of ln σ vs $1/T$ (inset picture: activation energy of different composite membranes).

To obtain further information about the proton-transport mechanism, we studied the activation energy of different composite membranes. As shown in Figure 6b, the relationship between the temperature and conductivities met the Arrhenius law as follows:

$$\sigma = \sigma_0 \exp\left(-\frac{E_a}{RT}\right) \quad (1)$$

where E_a is the activation energy, kJ mol^{-1}; σ is the conductivity, S cm^{-1}; R is the universal gas constant (8.314 J mol^{-1} K^{-1}), and T is the absolute temperature, K.

It can be seen that the addition of [dema][TfO] decreased the E_a value because of the enhanced free ionic mobility. The calculated E_a values ranged from 14 to 27 kJ mol^{-1}, which was between the activation energy of the Grottuss mechanism, ranging from 14 to 40 kJ mol^{-1},[42] implying that the form of proton transfer in this IL-based membrane could be dominated by this mechanism. One possible hypothesis is that the H−N bond from the ammonium cation of [dema][TfO] could interact with the C═N bond of PBI and proton conduction probably involves transfer from ammonium to C═N to C═N to amine, etc. However, with a higher content of [dema][TfO], the presence of free IL in the membrane was observed by DSC and these free IL can improve the ion conductivity. As we know, the water-swelled electrolyte membrane has two kinds of proton-transfer mechanisms, namely, proton hopping (Grotthuss mechanisms) and diffusion (vehicular mechanisms).[43] In this case, proton transport might have occurred by both of the two mechanisms. When the content of [dema][TfO] was lower, proton transport might have occurred predominantly by hopping mechanisms, and via diffusion was restricted, because the free IL in the membrane facilitating proton diffusion was limited. This situation was similar to proton transport in water-swelled electrolyte membranes under low-humidity conditions. With a higher content of [dema][TfO], there existed free protic IL, which could be used as a proton conductor to improve the conductivity (vehicular mechanism). Figure 7 gives a schematic diagram of ion conduction hypothesis in the composite membrane.

Figure 8 presents the conductivity changes of composite membranes with time. Contrary to that reported in the literature,[24,25] the conductivity did not decrease dramatically. After 400 h, the conductivity of PBI/[dema][TfO]80 and PBI/[dema][TfO]83 composite membranes only reduced by 18% and 10%, respectively. The conductivity was still sufficient for anhydrous requirements at high temperature. This was because

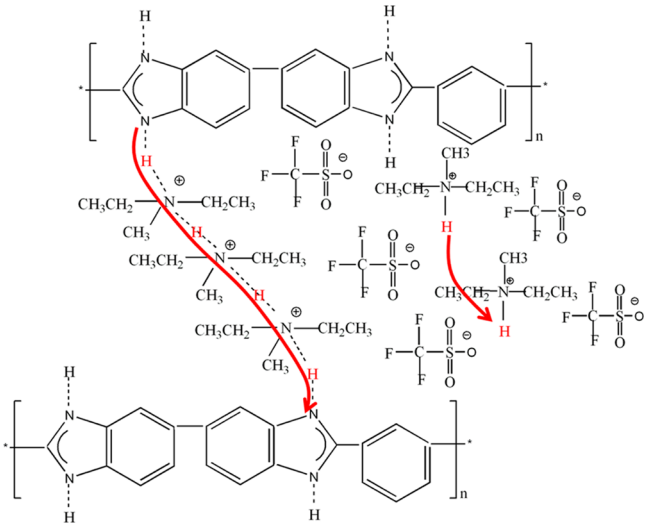

Figure 7. Hypothesis of ion conduction in the IL-based membrane.

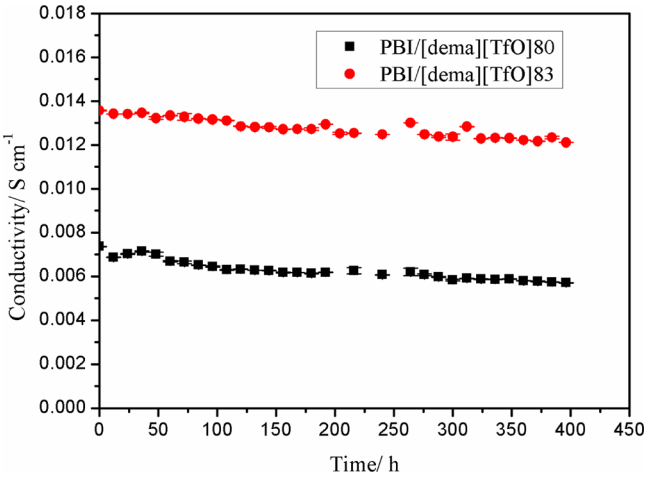

Figure 8. Time-dependent proton conductivities of composite membranes at 120 °C.

most of the IL was entrapped in the polymer matrix by the ionic interaction described above.

The H_2/Cl_2 fuel cell prepared using a PBI/[dema[TfO]83 hybrid membrane with a thickness of 80 μm was operated at 120 and 140 °C without humidification. As shown in Figure 9, the cell gave the highest power density of 26.50 and 29.64 mW cm^{-2} at 120 and 140 °C, respectively. We also tested the hydrogen-permeation current density of the hybrid membrane, and it was only 0.4 mA cm^{-2}, which was lower than that of the Nafion membrane.

In H_2/O_2 PEMFC, some reports[20] suspected that a small amount of the IL was leaked into the catalyst and formed the proton-conducting path with the water generated during the operation. However, in the H_2/Cl_2 fuel cell, there was no water, so the platinum catalyst was not fully utilized. Furthermore, the adhesion between the membrane and GDE was not sufficient at present. To solve these problems, optimization of the GDE structure and the three-phase reaction zone was necessary.

CONCLUSIONS

In this work, an IL-based proton-conducting membrane was proposed and designed for H_2/Cl_2 fuel cells. [dema][TfO] showed good thermal property, high ionic conductivity, and

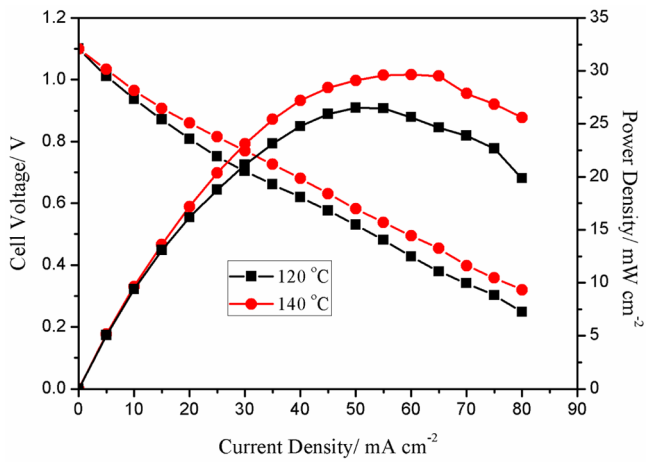

Figure 9. Polarization curve of an anhydrous H_2/Cl_2 fuel cell using the PBI/[dema][TfO]83 composite membrane at different temperatures.

good hydrogen and chlorine electrode kinetics. A PBI/[dema][TfO] composite membrane was prepared with good thermal and chemical stabilities, processability, and high conductivity. The Grotthuss and diffusion mechanism of proton transport may exist together in this composite membrane. Although the performance of the H_2/Cl_2 fuel cell still needs to be improved, we believe that our work provides an effective way for the development of a novel proton-conductive membrane for H_2/Cl_2 fuel-cell application.

ASSOCIATED CONTENT

Supporting Information

Comparison of anhydrous proton conductivity of the prepared membrane, CV curves, and experimental details. This material is available free of charge via the Internet at http://pubs.acs.org.

AUTHOR INFORMATION

Corresponding Authors

*E-mail: zhouli@dicp.ac.cn. Tel.: +86-411-84379123. Fax: +86-411-84379185.

*E-mail: zhgshao@dicp.ac.cn. Tel.: +86-411-84379153. Fax: +86-411-84379185.

Notes

The authors declare no competing financial interest.

ACKNOWLEDGMENTS

This work was financially supported by National High Technology Research and Development Program of China (863 Program, Grant 2012AA052002) and the National Basic Research Program of China (973 Program, Grant 2012CB215500).

REFERENCES

(1) Debe, M. K. *Nature* **2012**, *486*, 43−51.
(2) Foerster, F.; Nobis, A.; Stotzer, H. *Z. Elektrochem.* **1923**, *29*, 64−79.
(3) Schmid, A. *Helv. Chim. Acta* **1924**, *7*, 370−373.
(4) Thomassen, M.; Borresen, B.; Hagen, G.; Tunold, R. *Electrochim. Acta* **2005**, *50*, 1157−1167.
(5) Gileadi, E.; Srinivasan, S.; Salzano, F. J.; Braun, C.; Beaufrere, A.; Gottesfeld, S. *J. Power Sources* **1977/78**, *2*, 191−200.
(6) Thomassen, M.; Anderson, E.; Borresen, B.; Tunold, R. *J. Appl. Electrochem.* **2006**, *36*, 813−819.

(7) Yeo, R. S.; Mcbreen, J.; Tseung, A. C. C.; Srinivasan, S. *J. Appl. Electrochem.* **1980**, *10*, 393−404.
(8) Hsueh, K. L.; Chin, D.-T. *J. Appl. Electrochem.* **1981**, *11*, 503−515.
(9) Liu, S.; Yu, H. M.; Zhou, L.; Wang, P. J.; Shao, Z. G.; Yi, B. L. *Int. J. Hydrogen Energy* **2012**, *37*, 11425−11430.
(10) Liu, S.; Zhou, L.; Wang, P. J.; Zhang, L. S.; Shao, Z. G.; Yi, B. L. *J. Mater. Chem.* **2012**, *22*, 20512−20519.
(11) Anderson, E. B.; Taylor, E. J.; Wilemski, G.; Gelb, A. *J. Power Sources* **1994**, *47*, 321−328.
(12) Thomassen, M.; Borresen, B.; Scott, K.; Tunold, R. *J. Power Sources* **2006**, *157*, 271−283.
(13) Mader, J. A.; Benicewicz, B. C. *Macromolecules* **2010**, *43*, 6706−6715.
(14) Han, M.; Zhang, G.; Liu, Z.; Wang, S.; Li, M.; Zhu, J.; Li, H.; Zhang, Y.; Lew, C. M.; Na, H. *J. Mater. Chem.* **2011**, *21*, 2187−2193.
(15) Welton, T. *Chem. Rev.* **1999**, *99*, 2071−2084.
(16) Wasserscheid, P.; Keim, W. *Angew. Chem., Int. Ed.* **2000**, *39*, 3772−3789.
(17) Plechkova, N. V.; Seddon, K. R. *Chem. Soc. Rev.* **2008**, *37*, 123−150.
(18) Chen, G.; Wei, B.; Luo, Y.; Logan, B. E.; Hickner, M. A. *ACS Appl. Mater. Interfaces* **2012**, *4*, 6454−6457.
(19) Susan, M. A. B. H.; Kaneko, T.; Noda, A.; Watanabe, M. *J. Am. Chem. Soc.* **2005**, *127*, 4976−4983.
(20) Lee, S.-Y.; Ogawa, A.; Kanno, M.; Nakamoto, H.; Yasuda, T.; Watanabe, M. *J. Am. Chem. Soc.* **2010**, *132*, 9764−9773.
(21) Lu, F.; Gao, X.; Yan, X.; Gao, H.; Shi, L.; Jia, H.; Zheng, L. *ACS Appl. Mater. Interfaces* **2013**, *5*, 7626−7632.
(22) Mannarino, M. M.; Liu, D. S.; Hammond, P. T.; Rutledge, G. C. *ACS Appl. Mater. Interfaces* **2013**, *5*, 8155−8164.
(23) Ke, C. C.; Li, J.; Li, X. J.; Shao, Z. G.; Yi, B. L. *RSC Adv.* **2012**, *2*, 8953−8956.
(24) Che, Q.; He, R. H.; Yang, J. S.; Feng, L.; Savinell, R. F. *Electrochem. Commun.* **2010**, *12*, 647−649.
(25) Ye, Y. S.; Cheng, M. Y.; Tseng, J. Y.; Liang, G. W.; Rick, J.; Huang, Y. J.; Chang, F. C.; Hwang, B. *J. Mater. Chem.* **2011**, *21*, 2723−2732.
(26) Yasuda, T.; Nakamura, S.; Honda, Y.; Kinugawa, K.; Lee, S. Y.; Watanabe, M. *ACS Appl. Mater. Interfaces* **2012**, *4*, 1783−1790.
(27) Liu, S.; Zhou, L.; Wang, P. J.; Shao, Z. G.; Yi, B. L. *J. Mater. Chem. A* **2013**, *1*, 4423−4426.
(28) Pu, H. T.; Liu, L.; Chang, Z. H.; Yuan, J. J. *Electrochim. Acta* **2009**, *54*, 7536−7541.
(29) Li, J.; Li, X.; Zhao, Y.; Lu, W.; Shao, Z.; Yi, B. *ChemSusChem* **2012**, *5*, 896−900.
(30) Yasuda, T.; Ogawa, A.; Kanno, M.; Mori, K.; Sakakibara, K.; Watanabe, M. *Chem. Lett.* **2009**, *38*, 692−693.
(31) Susan, M. A. B. H.; Noda, A.; Mitsushima, S.; Watanabe, M. *Chem. Commun.* **2003**, 938−939.
(32) Nakamoto, H.; Watanabe, M. *Chem. Commun.* **2007**, 2539−2541.
(33) Susan, M.; Kaneko, T.; Noda, A.; Watanabe, M. *J. Am. Chem. Soc.* **2005**, *127*, 4976.
(34) He, Y.; Lodge, T. P. *Chem. Commun.* **2007**, 2732−2734.
(35) Sekhon, S. S.; Park, J.-S.; Cho, E.; Yoon, Y.-G.; Kim, C.-S.; Lee, W.-Y. *Macromolecules* **2009**, *42*, 2054−2062.
(36) Mondal, A. N.; Tripathi, B. P.; Shahi, V. K. *J. Mater. Chem.* **2011**, *21*, 4117−4124.
(37) Shimano, S.; Zhou, H.; Honma, I. *Chem. Mater.* **2007**, *19*, 5216−5221.
(38) Johnson, L.; Ejigu, A.; Licence, P.; Walsh, D. A. *J. Phys. Chem. C* **2012**, *116*, 18048−18056.
(39) Mamlouk, M.; Ocon, P.; Scott, K. *J. Power Sources* **2014**, *245*, 915−926.
(40) Wang, J. T.-W.; Hsu, S. L.-C. *Electrochim. Acta* **2011**, *56*, 2842−2846.
(41) Chuang, S. W.; Hsu, S. L. C. *J. Polym. Sci. A* **2006**, *44*, 4508−4513.
(42) Yu, S. M.; Yan, F.; Zhang, X. W.; You, J. B.; Wu, P. Y. i.; Lu, J. M.; Xu, Q. F.; Xia, X. W.; Ma, G. L. *Macromolecules* **2008**, *41*, 3389−3392.
(43) Cho, E. K.; Park, J. S.; Sekhon, S. S.; Park, G. G.; Yang, T. H.; Lee, W. Y.; Kim, C. S.; Park, S. B. *J. Electrochem. Soc.* **2009**, *156*, B197−B202.